Arch. Metall. Mater. **68** (2023), 2, 791-798

DOI: https://doi.org/10.24425/amm.2023.142463

RAJESH PUROHIT[1], M.M.U. QURESHI[1], ASHISH KUMAR[1*], ABHISHEK MISHRA[1], R.S. RANA[1]

FABRICATION AND CHARACTERIZATION OF Al6061-NANO Al_2O_3 COMPOSITES BY ULTRASONIC ASSISTED STIR CASTING FOLLOWED BY HEAT TREATMENT AND HOT FORGING

The present work comprises the development of Al6061/nano Al_2O_3 composites with 0 to 4 weight percent in steps of 0.5 wt. % of nano alumina particles by using ultrasonic assisted stir casting. Casted samples were subjected to heat treatment and hot forging. Further forged and heat-treated gear blanks of nano Al_2O_3 (0 to 3.0 weight %) reinforced nanocomposites were machined to make spur gears for the wear test. The results have shown that nano Al_2O_3 reinforcement in the Al6061 matrix with heat treatment and forging improves the hardness and compressive strength up to 3.5 wt. %, after that, it starts decreasing because of the agglomeration of nano alumina particles. SEM results reveal grain refinement of the pure alloy after reinforcement. Removal of porosity and voids observed after forging operation. Wear resistance increasing with incorporation of Al_2O_3 nanoparticles in base alloy, reinforcement wt. %, precipitation hardening and hot forging also improves wear resistance and mechanical properties. These composites have widespread applications in gear, brake discs, crankshaft, clutch plates, pistons, and other components of automobiles and aircraft structures.

Keywords: Al6061 Alloy; Al6061-Al_2O_3 nanocomposites; XRD analysis; FESEM; Mechanical Properties; Automotive gears

1. Introduction

Composite materials are made up of two or more materials with a unique arrangement of properties not available in the base materials. They are different from alloys because both components stay distinct and identifiable in the finished component and are free from the restrictions offered by the thermodynamic equilibrium diagram. Some composite materials include brake discs, connecting rods, pistons, fiberglass, mud bricks, and natural composites such as bones, granite, and wood. The nanocomposites are materials with reinforcement having one, two, or three dimensions less than 100 nm or having nano-scale microstructural features inside their body structures [1,2]. The material with more than one phase, where one phase is the matrix and the other is reinforcement, which is dispersed in a matrix phase, is known as composite material [3-5]. Materials used for matrix and reinforcement purposes have different properties, and after mixing, the resultant composite material shows different properties from the individual constituent materials. Generally, the discontinuous or stronger phase is known as the reinforcement phase, and the continuous or weaker phase is called the matrix phase [6].

Nanocomposites of the metal matrix (MMNC) are the materials where the base matrix belongs to the metal, and the rest may be metal or non-metal like ceramic. The percentage of reinforced nanoparticles in metal matrix composites is generally 0 to 5 wt.%. The processing of metal matrix nanocomposites is the casting route, powder metallurgy route, and other new processing techniques [6,7]. Nanocomposites of metal matrix (MMNC) includes Al5083/TiC, Al/Al_2O_3, Al/SiC/, Al/TiO_2 etc. Rajkumar et al. [8] analyzed the changes in hardness behavior after the addition of SiC particles in Al-Si alloy using stir casting route, they found a significant increment in hardness value with reinforcement attributed to the hard nature of SiC.

Nayak and Date et al. [9] presented the studies on different types of AMCs, i.e., Al-3 vol. & Al-7 wt. % SiC and Al-3 vol. & Al-7 vol. % Al_2O_3-composite fabricated by powder metallurgy process. One-step deformation was accomplished at 500°C temperature at strain rates of 10 & 20 per second. In a two-step deformation, the first deformation at 500°C and the second deformation at 430°C at strain rates of 10 & 20 per second, respectively. The outcome of hot compression on all four composite samples found that the heat-treatment of composites exhibited lower porosity, improved density, and increased hardness. Other

[1] MECHANICAL ENGINEERING DEPARTMENT, MANIT, BHOPAL, INDIA-462003

* Corresponding author: bhaskar.171ashish@gmail.com

researchers have done work on Al6061-composites reinforced with Ni-coated 8 wt. % TiO_2 particles made by stir casting. The hot forging was performed at 500°C with a deformation ratio of 6:1 on aluminum Al6061-TiO_2 composites. Microhardness and tensile tests revealed that the TiO_2 reinforcement in the Al6061 enhances the micro-hardness and UTS of the composites. A micrograph study shows hot forging results in uniform microstructure and an upsurge in mechanical properties [10-13]. Incorporating ceramic SiC particles in al alloy improves the mechanical and tribological properties, and wear resistance is significantly enhanced with the addition of reinforcement [14,15].

Current research includes the fabrication of Al6061/Al_2O_3 nanocomposites. Later the heat treatment and hot forging were performed on the developed composites. The effect of heat treatment and hot forging was analyzed with the help of mechanical, metallographic, and tribological characterization in comparison with as-cast alloy and composites.

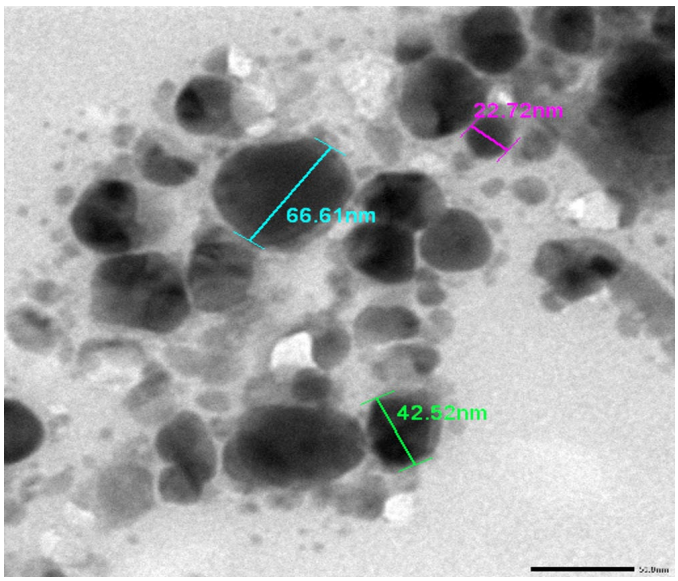

Fig. 1. TEM Image of Nano Al_2O_3 Particles

2. Materials and methods

2.1. Selection of material

Al-Mg-Si (Al 6061) alloy was selected as the matrix, and nano Al_2O_3 particles were incorporated as reinforcement to develop the nanocomposites. AA6061 is a most common heat-treatable Al-alloys and has excellent mechanical properties. The compositions of Al6061 alloy (purchased from Paraswamani metals, Mumbai) and nano Al_2O_3 particles (Purchased from Nano Shell, USA) are given in TABLES 1 and 2, respectively, as provided by the company. The SEM of Al_2O_3 nanoparticles are shown in Fig. 1, procured from Nano Shell, India.

2.2. Fabrication of nanocomposites

The casting of Al-Al_2O_3 nanocomposites was done on the Ultrasonic Assisted stir casting method. The weighted amount of Al-6061 alloy was liquefied in the graphite crucible in the programmable electric resistance furnace at 760°C, and dry N_2 gas was used for degassing. Then preheated (300°C) nano Al_2O_3 particles were introduced into the molten alloy, and mixing through a metallic stirrer was performed for 10 minutes at 450 rpm. Then ultrasonication with the help of a niobium probe was done for 5 minutes. After that, it was immediately dispensed in the preheated mold. The solidified casting was taken out after cooling down. Similar procedures were adopted for casting Al nano Al_2O_3 composite samples with 0, 0.5, 1, 1.5, 2, 2.5, 3, 3.5, and 4 wt. % of nano Al_2O_3 particles.

2.3. Heat treatment and forging

The T-6 heat treatment of cast and hot forged samples of Al-nano Al_2O_3 composites using a muffle furnace. In this process, solution treatment was done at 530°C for 2 hours, followed by quenching in an oil bath. Later artificial aging was performed in which specimens were reheated to 175°C for 8 hours, followed by natural cooling in still air.

The Al-Al_2O_3 nanocomposite (0.5 to 4 wt. % of nano alumina) specimens (50 mm diameter and 110 mm length) were heated to 500 ± 3°C for 1 h. Then they were hot forged on a hydraulic press at Hari Engineering Industries, Govindpura, Bhopal, India. The force was applied up to 800 KN, and the workpiece was pressed to the final length of 70 mm. Fig. 4.10 and 4.11 show the hot forging of Al-Al_2O_3 nanocomposite samples to test properties during forging. Figs. 2 and 3 show the nanocomposite samples before and after forging, respectively.

TABLE 1

Elemental Investigation of Al 6061 alloy

Element	Si	Fe	Cu	Mn	Pb	Ni	Zn	Ti	Sn	Mg	Cr	Al
Percentage	0.43	0.7	0.24	0.139	0.24	0.05	0.25	0.15	0.001	0.802	0.25	96.748

TABLE 2

Composition of Al_2O_3 nanoparticles

Element	Al_2O_3	Si	Na	K	Fe	Cu	Ti	Mn
Composition (PPM)	99 + %	10.8	9.01	10.6	9.75	0.12	0.86	0.72

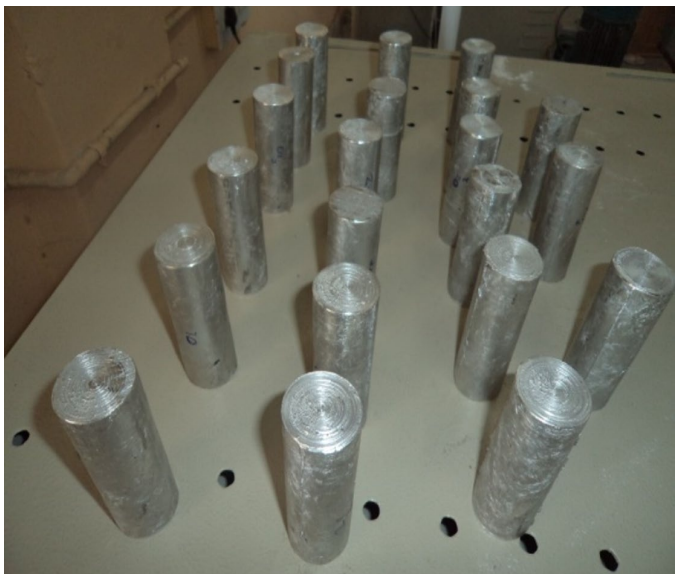

Fig. 2. Un-forged samples

Fig. 3. Samples after hot forging

Fig. 4. Manufactured Al-nano Al_2O_3 composite spur gears

The hot forged and heat-treated Al-nano Al_2O_3 composite billets were cut into gear blanks of about 70 mm diameter. The spur gears were machined on the universal milling machine. The final dimensions of the machined spur gears include a 50 mm Pitch circle diameter (D), 29 teeth (T), and a 1.72 mm module. Fig. 4 shows the photograph of the final manufactured Al-Al_2O_3 nanocomposite Spur-gears with different compositions. The hardness of cast, heat-treated, and forged & HT Al6061-nano Al_2O_3 composites was tested in B-scale on a Rockwell-hardness tester. Readings were taken at five points, and mean values were stated. Rule of Mixture (ROM) found the theoretical density of Al nano Al_2O_3 composites.

3. Results and discussion

3.1. Microstructure analysis

FESEM is carried out for the analysis of the microstructure of nanocomposites. Fig. 5(a-c) depicts the microstructure of 0.5, 1.5, and 2.5 wt.% alumina nanocomposites in the as-cast

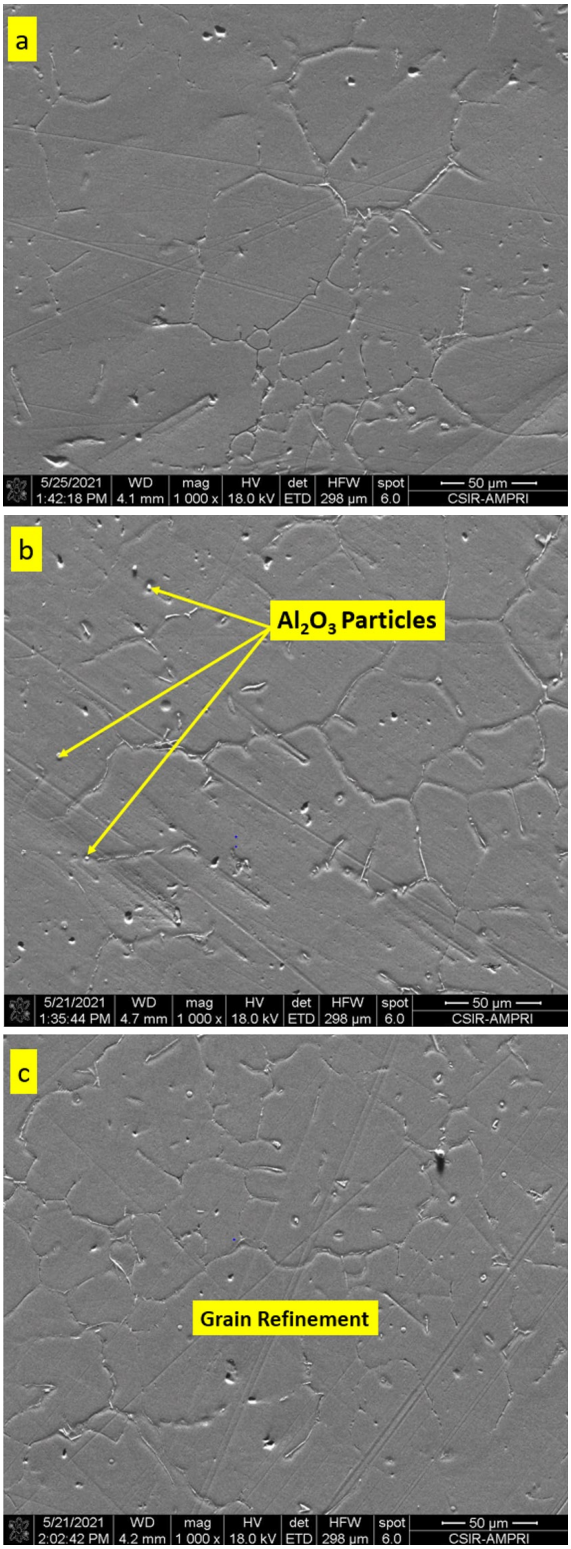

Fig. 5. FESEM image of unforged and As cast nanocomposites (a) 0.5 wt. % Al_2O_3, (b) 1.5 wt. % Al_2O_3, (c) 2.5 wt. % Al_2O_3

condition. Alumina reinforcement is successfully embedded and detected between the pure aluminum alloy matrix. It is also observed that the grain size of composite is minimized after increasing the weight percentage of nano alumina. The refinement of grains might be due to hard particles at grain boundaries hindering grain growth; as the number of particles increases in the matrix, due to this phenomenon, the number of grains increases with the weight percentage of alumina. Fig. 6(a-c) shows the EDS spectrum of 0.5, 1.5 and 2.5 wt. % nanocomposites. The increasing alumina can be seen from 0.5 to 2.5 wt. % composites. EDS identified the major alloying elements and reinforcing content. Fig. 7(a-c) shows the FESEM image of forged and heat-treated nanocomposite samples varying from 0.5 to 2.5 wt. % nano alumina. Mg_2Si is the major precipitate formed after heat treatment and can be seen in the microstructure. These precipitates are formed after the specimen's artificial aging contributes to the strength and hardness improvement. The grains are significantly compressed after the performance of forging. The amount of void content and porosity also decreased after the forging operation. The micrographs did not show any pullout of

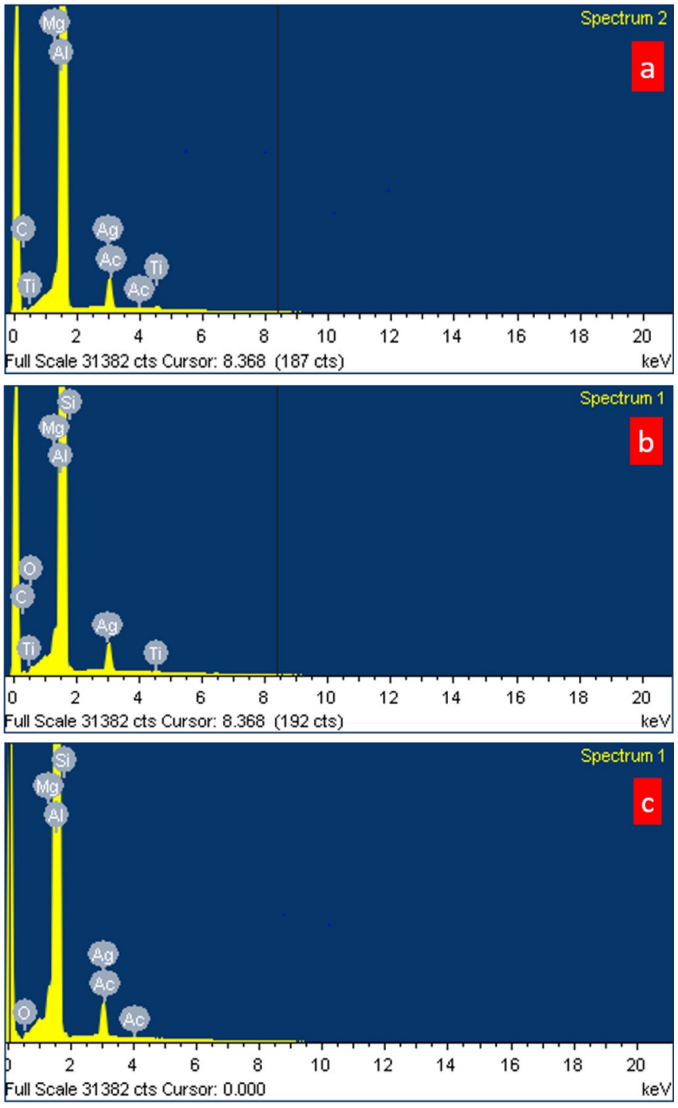

Fig. 6. EDS Spectrum of unforged and As cast nanocomposites (a) 0.5 wt. % Al_2O_3, (b) 1.5 wt. % Al_2O_3, (c) 2.5 wt. % Al_2O_3

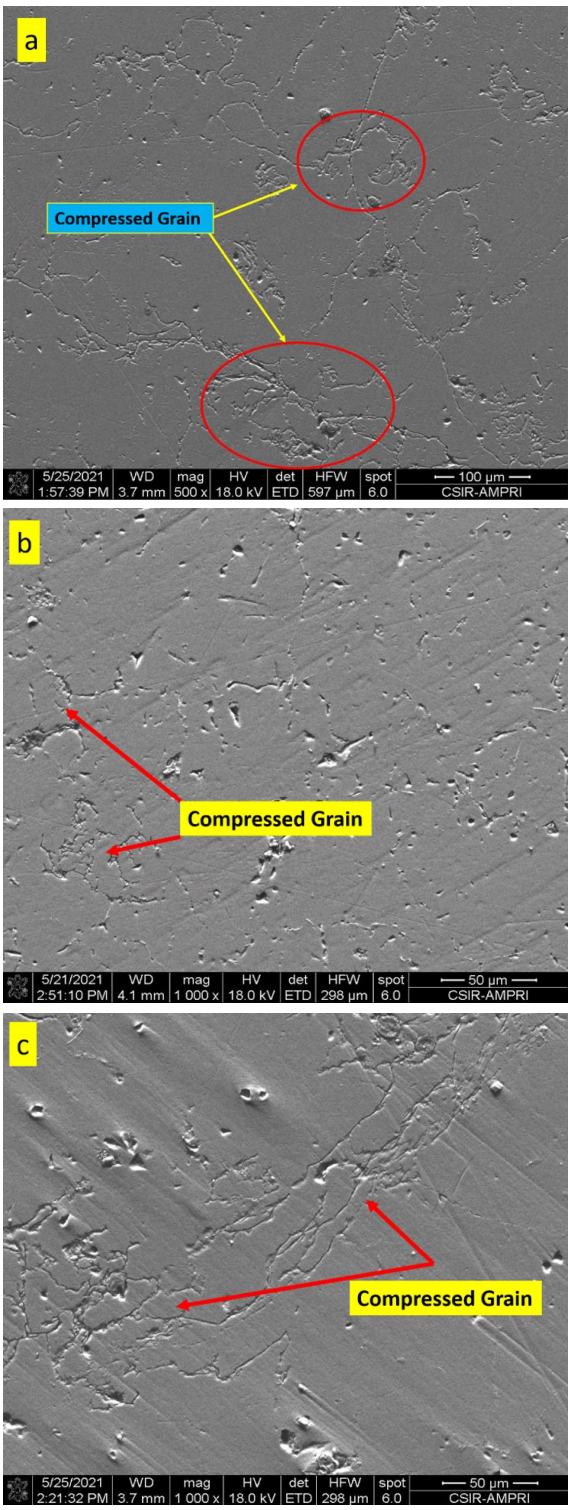

Fig. 7. FESEM image of forged and Heat treated nanocomposites (a) 0.5 wt. % Al_2O_3, (b) 1.5 wt. % Al_2O_3, (c) 2.5 wt. % Al_2O_3

particles after forging, reflecting good bonding between matrix and Nano alumina reinforcement.

3.2. XRD analysis

The formation of the nanocrystalline phase of the Al6061 metal matrix reinforced with nano Al_2O_3 is confirmed with the

crystalline phase of combustion-derived Al_2O_3. The XRD pattern of Al_2O_3 powder shows the crystalline nature having a rhombohedra crystal structure, and the parameters of the crystalline cell are a = 4.7587 Å, b = 4.7587 Å, and c = 12.9929 Å. The diffraction peaks of the Al_2O_3 crystalline phase are indexed to (110), (113), (122), and (208) reflections.

The broadening of the reflections indicates the inherent nature of nanocrystals. The XRD result of Fig. 8 displays the crystalline concentrations, peaks position, shape, and width. Which provides essential information about the arrangement of the Al6061 reinforced with 0.5 wt. % nano Al_2O_3 of forged and heat-treated sample. Peaks have been obtained in the 2q span ranging from 20 to 100 degree and the peaks at 2Θ of 38.73°, 44.94°, 65.31°, and 78.41° belongs to Pure Al, and the peaks at 2Θ of 35.26°, 42.23°, 57.56°, and 75.42° belong to Al_2O_3 and other remaining minor peaks attributed to impurity. The peaks of Al_2O_3 are clearly shown at near 2q angle 36°, 41°, 56°, and 77°. Fig. 9 shows an XRD graph of forged and a heat-treated sample of Al6061-2.5 wt. % nanoAl_2O_3 composites. The peaks of reinforced particles appear almost the same as of forged and heat-treated Al-6061-0.5 wt. % Al_2O_3 nanocomposite sample. The peaks have been obtained in the 2q span ranging from 20 to 100 degree and the peaks at 2Θ of 38.73°, 44.94°, 65.25° belongs to pure Al, and the peaks at 2Θ equal to 36.46°, 44.67°, 59.2° and 69.2° belongs to Al_2O_3 and other remaining minor peaks attributed to impurity.

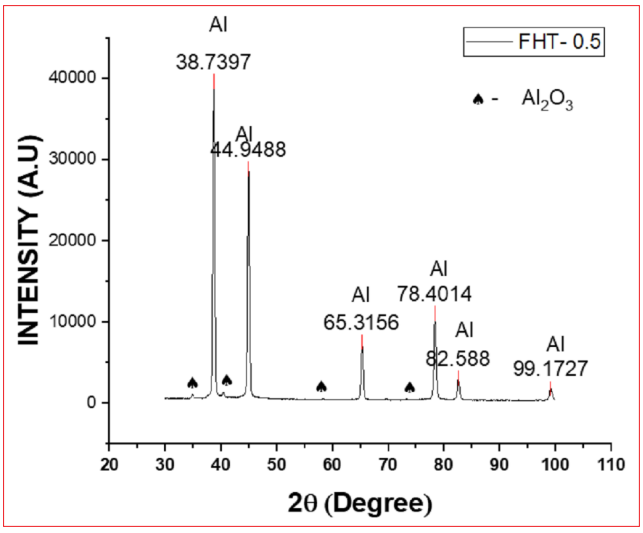

Fig. 8. XRD graph of forged & heat-treated (FHT) Al6061/0.5 wt. % nano Al_2O_3 Composite sample

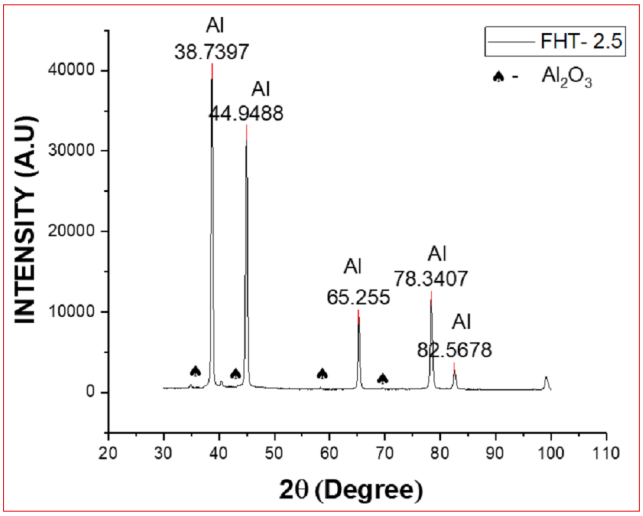

Fig. 9. XRD graph of forged & heat-treated (FHT) Al6061/2.5 wt. % nano Al_2O_3 Composite sample

3.3. Density measurement and Porosity content

Fig. 10 shows the theoretical and actual density of cast and forged nanocomposites. From the figure, it is observed that theoretical density steadily surges with the rise in wt. % of nano alumina particles due to the higher density of nano alumina particles than the Al 6061 alloy. It is also seen that the actual density of forged samples is more than the as-cast samples, which ensures that the forging results in densification due to grain refinement and reduction of various casting defects like blow holes, porosity, micro-cracks etc.

The porosity of the Al-Al_2O_3 nanocomposites was determined by measuring the actual and theoretical densities of the different samples. Fig. 11 shows the porosity variation of Al-nano Al_2O_3 composites with wt. % of nano alumina particulates for the as-cast and forged samples. It shows that the porosity upsurges

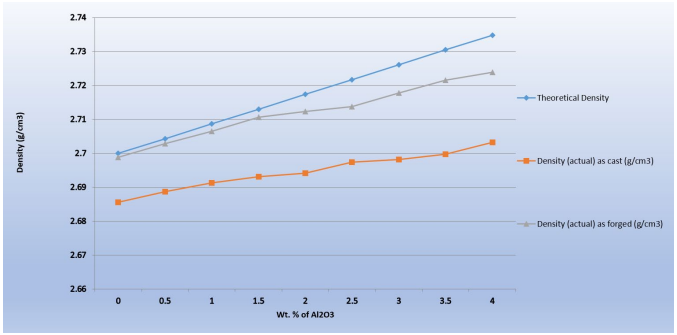

Fig. 10. Variation of the theoretical and measured density of alloy and nanocomposites

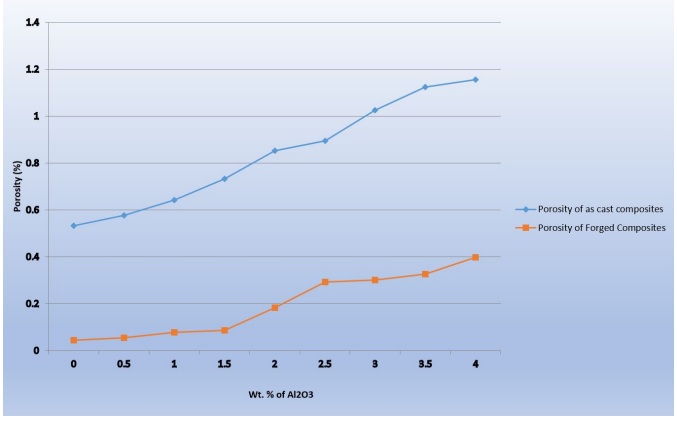

Fig. 11. Porosity variation of as-cast and hot forged alloy and nanocomposites

with the rise in wt. % of nano alumina attributed to the lower wettability and agglomeration of particles at higher wt. % of nano alumina, nucleation of pores at the aluminum and Al_2O_3 interfaces, and difficulty in the flow of molten metal due to particle clusters lead to porosity formation [16,17]. It shows that the porosity is significantly decreased after hot forging maximum up to 91.67% attributed to the densification and grain refinement of matrix alloy. This also confirms that the hot forging made it possible to reduce the various casting defects like blow holes, micro-porosity, voids etc.

3.4. Hardness

The hardness of as-cast, heat-treated, and forged & heat-treated Al-Al_2O_3 nanocomposites is depicted in Fig. 12. The hardness values were found to increase with the increase in weight % of nano alumina up to 3.5 wt. %, after which it starts decreasing. The increase in hardness of nanocomposite is attributed to the combined effect of the hard nature of alumina particle, grain refinement, increased dislocation density by the difference in thermal coefficient of the matrix, and reinforcement creating a hindrance to the dislocation movement. The hardness decreases after 3.5 wt. % attributed to clustering of nanoparticles at greater weight percent, due to that indentation value fluctuated from region to region, and the overall value decreased. Fig. 12 also shows that the hardness of Al6061-nano Al_2O_3 composites increases by heat treatment and forging of the nanocomposites. The results have a similar trend as reported by other researchers [18-20]. The forging increases hardness due to grain refinement, strain hardening effect, decrease in porosity, higher densification, and improvement in bonding between matrix and reinforcement particles. Compared to un-reinforced alloy, Al-3.5 wt. % Al_2O_3 nanocomposites' hardness was found to increase by 6.17%, 8.0%, and 8.47% in as-cast, heat-treated, and the forged & heat-treated conditions respectively.

3.5. Compressive strength

Fig. 13 shows the variation of compressive strength (MPa) with wt. % of nano Al_2O_3 particles for the as-cast, heat-treated (HT), and forged & HT samples of Al-Al_2O_3 nanocomposites. The figure shows that the compressive strength upsurge with wt. % of Al_2O_3 nanoparticles up to 3.5 wt. % after which it decreases. The increase in compressive strength with wt. % of nano alumina particles is attributed to an increase in work hardening rate with higher wt. % of nanoparticles and the hard nano alumina particles act as an obstacle to dislocation movement. The compressive strength decreases after 3.5 wt. % due to the formation of bundles of nanoparticles and agglomeration at greater wt. % and increase in microstructural defect and micro-porosity, i.e., voids above 3.5 wt. % due to the higher surface energy of nanoparticles. Fig. 13 also shows that the compressive strength increases with the heat treatment and forging to nanocomposites.

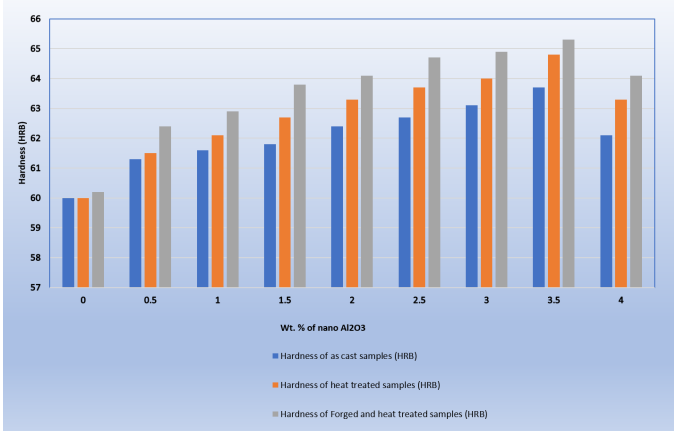

Fig. 12 Variation Hardness with wt. % of nano Al_2O_3 for as cast, heat-treated, and Forged & heat-treated samples

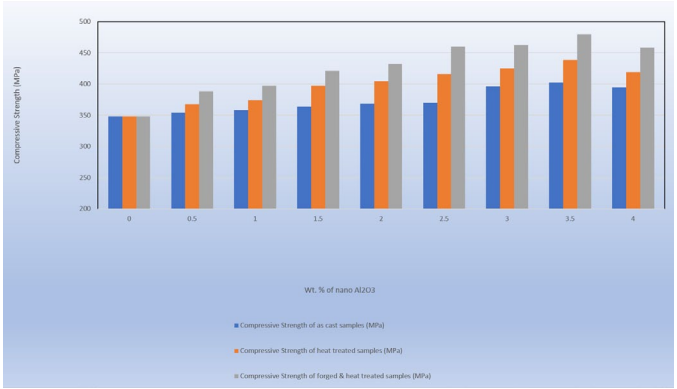

Fig. 13. Variation of compressive strength of Al- Al_2O_3 nanocomposites with wt. % of nano alumina for as cast, heat-treated, and forged & HT conditions

As compared to un-reinforced alloy, compressive strength of Al-3.5 wt. % Al_2O_3 nanocomposites were found to increase by 15.63%, 26.06%, and 37.81% in as-cast, heat-treated & the, forged, and heat-treated conditions, respectively. The compressive strength increases after forging due to the grain refinement, porosity reduction, filling of micro-cracks, improvement in the distribution of nanoparticles, and strain hardening effect. Agglomeration of particles also decreases by the plastic deformation of the nanocomposite samples [16].

3.6. Wear characteristics

The wear test of hot forged and heat-treated Al-Al_2O_3 nanocomposite gears with 0-3 wt. % nano alumina was performed on the fabricated wear testing set-up. The wear tests were performed under 1 & 2 kg load for 1, 2 & 3 hours of test periods. Fig. 14 and 15 show the dry sliding wear test results at 1 and 2 kg load, respectively, for 1, 2, and 3 h. It is observed that the wear loss increases as the sliding distance increases due to plastic deformation. More wear was found after 3 hr compared to 1 and 2 h. As the reinforcement weight % increases from 0 to 3, the wear loss decreases for the same sliding distance; this

behavior shows that wear resistance improves with increasing the amount of Al_2O_3. This can be attributed to the increased load-bearing capacity, introduction of hard secondary phases, precipitation hardening, strengthening mechanisms, and uniform distribution of hard alumina particles in the Al alloy matrix [21]. The decreasing weight-loss trend was noticed from 0 to 3 wt.% because of hardness improvement with increasing ceramic nano Al_2O_3 in soft aluminum alloy. In contrast, weight loss increases with increasing siding distance or wear time from 1 h to 3 h for all compositions. The superior interfacial bond in the hot forged and heat-treated Al-nano alumina composite gears prevents the pullout of hard Al_2O_3 nano particulates from the Al-matrix, abolishing the possibility of 3-body wear and hence increase in wear resistance [22].

The wear loss results of pure alloy and Al alloy-Al_2O_3 nanocomposites at 2 kg load for 1, 2, and 3 h sliding duration are displayed in Fig. 15. From the analysis of the results, the weight loss increases with load from 1 kg to 2 kg. Wear loss for 0.5 wt. % at 2 kg for the different sliding duration, the wear increasing with increment in load from 1 kg to 2 kg comparting to Fig. 14. The resistance to wear increases with the amount of reinforcement. The resistance to wear improves with increasing weight % of nano alumina, and the load is dominant in the wear loss of composites for all compositions. The wear loss increases with the upsurge in load due to the formation of the high plastic-deformation region on sample surfaces, and delamination occurs

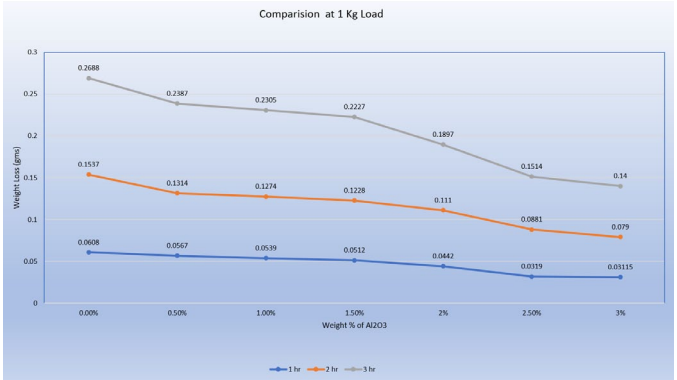

Fig. 14. Variation of wear loss with wt. % of nano alumina for Al-nano Al_2O_3 composite gears under 1 Kg load

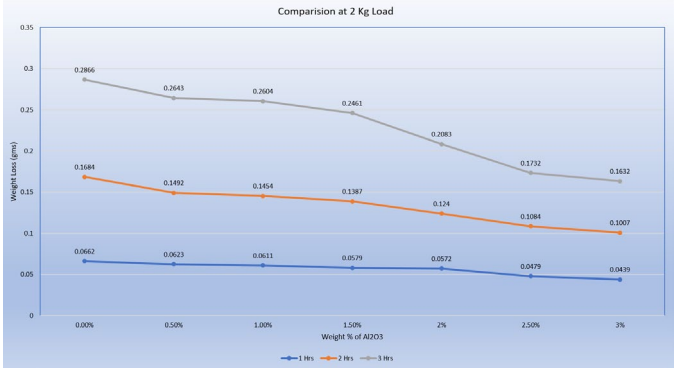

Fig. 15. Variation of wear loss with wt. % of nano alumina for Al-nano Al_2O_3 composite gears under 2 Kg load

at increased loads. During wear testing of gears, high speed and load cause fracture at the interfacial zones between reinforcement and the Al alloy, hence the higher wear loss. The results are in line with that reported by other researchers [23,24].

The wear loss decreases maximum up to 41.34% and 38.25% with an increase in wt. % of nano alumina from 0.5 to 3 wt. % for 1 and 2 kg load, respectively. From the wear analysis, it can be concluded that the adhesive wear mechanism strongly relates to wear at a lower load. But as the load increases, some reinforcing particles get de-bonded along with matrix material. These particles act as a third body between meshing gears; hence at higher loads, the wear of the specimen is strongly due to the three-body abrasion. Due to the low ductility of hard-alumina particles, they can endure stresses without plastic deformation or rupture at smaller loads. This has already been known that if we prevent the plastic flow of material at the counter surface, the wear resistance will be improved, and wear loss will be reduced. Alumina particulates can bear relatively more stress, and hence they can increase wear resistance**.**

4. Conclusions

1) The density of the Al-Al_2O_3 nanocomposites increases with an increase in the weight % of nano alumina particles due to the higher density of alumina than aluminum alloy. The hot forging of Al nano Al_2O_3 composites increases density and reduces porosity content due to grain refinement and filling blow holes, voids, and pinhole porosity as the casing defects. Porosity decreases up to 91.67% after forging.
2) Al-Al_2O_3 nanocomposites' hardness and compressive strength increased with the increase in weight % of nano-alumina particles up to 3.5 wt. % after that it starts to decrease.
3) Microstructural examination of Al-nano alumina composites using SEM reveals that the nano alumina particles are uniformly distributed in the Al6061 alloy at both as-cast and hot forged conditions. Micrographs of hot forged & HT samples depict better dispersion of nano-alumina particles & alumina clusters are reduced.
4) The wear-losses were found to decrease with increasing weight % of nano alumina and increase with sliding distance a load. Alumina particles can withstand relatively high stresses and effectively increase wear resistance. Higher-plastic-deformation region on the sample surfaces and the delamination-wear occurs with increased loads.

REFERENCE

[1] A.H. Nakagawa, M.N Gungor, Microstructure and Tensile Properties of Al2O3 Particle Reinforced 6061 Aluminum Cast Composite: Fundamental Relationships between Microstructures and Mechanical Properties of Metal Matrix Composites 127-143 (1989).

[2] K.K. Chawla, Composite Materials, (eBook). Springer, New York & Heidelberg Dordrecht, London. (2013).
DOI: https://doi.org/10.1007/978-0-387-74365-3

[3] L.H. Manjunatha, P. Dinesh, Studies on effect of heat treatment and water quench age hardening on microstructure, strength, abrasive wear behaviour of Al6061-MWCNT metal matrix composites, J. Acad. Indus. Res. **1** (10), 595-600 (2013).

[4] I. Özdemir, Ü. Cöcen, K. Önel, The effect of forging on the properties of particulate-SiC-reinforced aluminium-alloy composites, Composites Science and Technology **60** (3), 411-419 (2000).

[5] K. Wu, K. Deng, K. Nie, Y. Wu, X. Wang, X. Hu, M. Zheng, Microstructure and mechanical properties of SiCp/AZ91 composite deformed through a combination of forging and extrusion process, Materials & Design **31** (8), 3929-3932 (2010).

[6] H.N. Reddappa, K.R. Suresh, H.B. Niranjan, K.G. Satyanarayana, Studies on mechanical and wear properties of Al6061/Beryl composites, Journal of Minerals and Materials Characterisation and Engineering **11**, 704-708 (2012).

[7] M. Singla, D.D. Dwivedi, L. Singh, V. Chawla, Development of aluminium based silicon carbide particulate metal matrix composite, Journal of Minerals and Materials Characterization and Engineering **8** (06), 455-467 (2009).

[8] R.K. Singh, A. Telang, S. Das, The influence of abrasive size and applied load on abrasive wear of Al-Si–SiCp composite, Arab. J. Sci. Eng. (2021).
DOI: https://doi.org/10.1007/s13369-021-06349-1

[9] K.C. Nayak, P.P. Date, Hot deformation flow behavior of powder metallurgy based Al-SiC and Al-Al2O3 composite in a single step and two-step uni-axial compression, Materials Characterization **151**, 563-581 (2019).

[10] C.S. Ramesh, R. Keshavamurthy, B.H. Channabasappa, A. Ahmed, Microstructure and mechanical properties of Ni–P coated Si3N4 reinforced Al6061 composites, Materials Science and Engineering: A **502** (1-2), 99-106 (2009).

[11] S.K. Biswas, B.P. Bai, (Dry wear of Al-graphite particle composites, Wear **68** (3), 347-358 (1981).

[12] A. Sverdlin, Introduction to aluminum. George E. Totten y D. Scott MacKenzie, "Handbook of Aluminum", **1**, 1, CRC Press, First Ed. (2003).

[13] B. Venkataraman, G. Sundararajan, Correlation between the characteristics of the mechanically mixed layer and wear behaviour of aluminium, Al-7075 alloy and Al-MMCs, Wear **245** (1-2), 22-38 (2000).

[14] R.K. Singh, A. Telang, S. Das, Abrasive wear response of Al-Si – SiCp composite: Effect of friction heat and friction coefficient," nt. J. Mater. Res. 1–7 (2021).
DOI: https://doi.org/10.1515/ijmr-2020-7869

[15] R.K. Singh, A. Telang, S. Das, Abrasive wear behaviour of as-cast and heat-treated Al – Si – SiCp composite, Int. J. Mater. Res. (formerly Z. Metallkd.) **109**, 1–9 (2018).
DOI: https://doi.org/10.1515/ijmr-2020-7869 10.3139/146.111727

[16] P.D. Srivyas, M.S. Charoo, Role of Fabrication Route On The Mechanical And TribologicalBehavior Of Aluminum Metal Matrix Composites – A Review. Materials Today: Proceedings **5** (9), 20054-20069 (2018).

[17] T.G. Durai, K. Das, S. Das, Wear behavior of nano structured Al (Zn)/Al2O3 and Al (Zn)–4Cu/Al2O3 composite materials synthesized by mechanical and thermal process, Materials Science and Engineering A **471** (1-2), 88-94 (2007).

[18] L. Kunčická, T.C. Lowe, F. Davis, R. Kocich, M. Pohludka, Synthesis of an Al/Al2O3 composite by severe plastic deformation, Materials Science and Engineering A **646**, 234-241 (2015).

[19] H.R. Ezatpour, M. Torabi-Parizi, S.A. Sajjadi, Microstructure and mechanical properties of extruded Al/Al2O3 composites fabricated by stir-casting process, Transactions of Nonferrous Metals Society of China **23**, (5), 1262-1268 (2013).

[20] T.P. Bharathesh, C.S. Ramesh, R. Keshavamurthy, S.M. Verma, Effect of Hot Forging on Mechanical Characteristics of Al6061-TiO2 Metal Matrix Composite, Materials Today: Proceedings **2** (4-5), 2005-2012 (2015).

[21] H.R. Ezatpour, S.A. Sajjadi, M.H. Sabzevar, A. Chaichi, G.R. Ebrahimi, Processing map and microstructure evaluation of AA6061/Al2O3 nanocomposite at different temperatures, Transactions of Nonferrous Metals Society of China **27** (6), 1248-1256 (2017).

[22] R. Srinivasan, B.S. Babu, M.M. Shufiyan, A.M. Thoufeeq, S.M. Sanjay, S.K. Varman, Experimental investigation on tribological behaviour of aluminium hybrid metal matrix composites processed through stir cum squeeze casting technique, Materials Today: Proceedings **27** (P2), 1756-1760 (2020).

[23] V.K.V. Meti, R. Konaraddi, I.G. Siddhalingeshwar, Mechanical and tribological properties of AA7075 based MMC processed through ultrasound assisted casting technique. Materials Today: Proceedings 5 (11), 25677-25687 (2018).

[24] S. Mula, S.K. Pabi, C.C. Koch, P. Padhi, S. Ghosh, Workability and mechanical properties of ultrasonically cast Al–Al2O3 nanocomposites, Materials Science and Engineering A **558**, 485-491 (2012).